Sensors and Actuators B 227 (2016) 24–28

Contents lists available at ScienceDirect

Sensors and Actuators B: Chemical

journal homepage: www.elsevier.com/locate/snb

Power law fluid viscometry through capillary filling in a closed microchannel

N. Morhell*, H. Pastoriza

Laboratorio de Bajas Temperaturas, Centro Atómico Bariloche and Instituto Balseiro, Comisión Nacional de Energía Atómica, Av. Bustillo 9500, R8402AGP S. C. de Bariloche, Argentina

ARTICLE INFO

Article history:
Received 2 April 2015
Received in revised form
16 November 2015
Accepted 11 December 2015
Available online 13 December 2015

Keywords:
Microviscometer
Closed channel
Power law fluid
Non-Newtonian viscosity

ABSTRACT

In this work we analyze the capillary filling dynamics of non-Newtonian fluids that can be modeled with a power law constitutive equation. We solve the Poiseuille equations for an hydrophilic closed channel where capillary pressures drives the fluid in until a rest position given by the barometric pressure is reached. We show that this dynamics can be used to measure both the coefficient k and exponent n, that describes the power law fluid viscosity and we ran tests on Soda Lime Glass microchannels. Using a simple experimental setup with a USB Microscope and a custom image processing software we were able to measure the power law parameters of whole blood, wall varnish and DI water.

The exponents were also obtained from the velocity profiles inside the microchannel using a custom μPIV setup matching both results with those measured with a standard Brookfield Rotational Microviscometer.

1. Introduction

One of the ongoing challenges in fluid rheometry is to provide fast and accurate viscosity measurements using very low sample volumes. Since the 1980s this problem was approached by miniaturizing internal flow sensors like capillary viscometers, or external flow sensors like Stokes and Rotational Viscometers. The latter has become one of today's industry standards, as rotational devices with cone-plate geometry can be used to directly measure the shear stress τ by setting different shear rates γ, thus calculating the viscosity μ as the ratio between these two variables ($\mu = \tau/\gamma$).

The miniaturization of fluid containers has dropped the minimum volume sample required down to ~500 μl [1] and in order to scale further down, novel microfluidic approaches have raised over in the recent years [2]. Standard photolithography microfabrication techniques widely used in microelectronics are now being used to manufacture external flow sensors, oscillators with a viscosity dependant resonance frequency [3], or capillary driven flow inside microchannels [4–6]. While these devices may use 10 μl of sample volume, they rely on a fluid dynamics model with the viscosity embedded in one or more parameters. Not any fluid can be measured in every viscometer and special care must be taken when analyzing non-Newtonian fluids.

In their 2005 work, Strivastava et al. [7], proposed a capillary flow viscometer using a microfluidic chip and a video recorder setup. The fluid dynamics of a fluid drop driven by capillarity is described by Poiseuille equation where viscosity, capillary pressure and channel geometry are binded constants. Srivastava's chip uses two independent channels to measure the dynamics and the capillary pressure, but the main drawback is the need of a third and a fourth channel where a test fluid has to be inserted to calibrate the geometrical dimensions. In 2006 [8] they showed how the same chip could be used to measure non-Newtonian fluids whose viscosity followed a power law model, a.k.a. a power law fluid. They used a known solution for a power law Poiseuille equation and showed that they could measure them with the same experimental setup, although the need of a test calibration fluid persisted.

Following the concept of capillary viscometer on a microfluidic chip, we have previously shown [9] that the analysis of the capillary filling in a closed channel provides enough information to compute both capillary pressure and viscosity in a single channel device. Moreover, we show that controlling the accuracy of the chip fabrication process [10] avoids the need of a test fluid, an attractive feature for applications in point of care devices. In this work, we analyze the capillary filling flow of a power law fluid and solve the modified Poiseuille equations for the velocity profile and the mean velocity across the channel. Then, we verify the model by testing fluids with a known non-Newtonian behavior. First, we show the power law behavior by μPIV measurements, contrasting with a

* Corresponding author.
E-mail address: nadim@cab.cnea.gov.ar (N. Morhell).

http://dx.doi.org/10.1016/j.snb.2015.12.033
0925-4005/

commercial Rotational Microviscometer, and finally we obtain the power law viscosity parameters with our single channel design.

2. Theory: capillary filling of a power law fluid in a closed microchannel

The Ostwald de Waele power law constitutive equation is a simple model to describe the changes of viscosity with the flow shear rate. In this model the viscosity is given by [11]

$$\mu = k\dot{\gamma}^{n-1} \tag{1}$$

where the constant k is the viscosity at $\dot{\gamma} = 1\ s^{-1}$, and n the exponent of the power law. In this model three kinds of fluids are distinguished: a pseudoplastic or shear thinning fluid for $n < 1$, a dilatant fluid for $n > 1$ and a Newtonian fluid with constant viscosity for $n = 1$.

The capillary filling inside a microchannel, described by a power law Poiseuille equation, can be studied to explicitly determine both viscosity parameters k and n. Here we present the solution of a fully developed Poiseuille flow inside a closed microchannel.

2.1. Pipe flow of a power law fluid

When a power law fluid inside a circular pipe of radius R is set to a pressure difference dP/dx, the velocity profile $u(r)$ is given by [12]

$$u(r) = \frac{1}{1+(1/n)}\left(\frac{1}{2k}\frac{dP}{dx}\right)^{1/n}\left(R^{1+(1/n)} - r^{1+(1/n)}\right) \tag{2}$$

where it can be seen that for $n = 1$ the Newtonian parabolic profile is obtained. Fig. 1a shows the profile for pseudoplastic and dilatant fluids, respectively a flattened or stretched parabola. Thus, a fit over a velocity profile can be used to measure the power law index n of a fluid in a pipe flow.

Is is usually easier to determine the mean velocity with an experimental setup that follows the free surface meniscus across the channel. The cross section of microchannels in microfluidic devices is seldom circular and an equivalent hydraulic diameter D is calculated. Rewriting R as a function of the hydraulic diameter D, the mean velocity u is given by [13]

$$u = \frac{D}{2((1/n)+3)}\left(\frac{D}{4k}\frac{dP}{dx}\right)^{1/n} \tag{3}$$

Eq. (3) can also be used to calculate both viscosity parameters k and n, although the parameters remain binded to the pressure gradient dP/dx which has to be independently determined.

2.2. Capillary flow in a closed channel

If a power law fluid sample is placed at the entrance of an hydrophilic microchannel the fluid will enter driven by a capillary pressure P_c. In a channel with an inlet and an outlet, *an open channel*, the fluid slows down continuously with the pressure gradient $\frac{\Delta P}{x}$, where ΔP is just P_c and x the fluid column length highlighted by the meniscus position. In a *closed channel* (Fig. 1-b) with an inlet and no outlet, the fluid compresses the trapped air and slows down until a rest position L_f, where the compressed air pressure P_x compensates both atmospheric pressure P_0 and capillary pressure. In this case $\Delta P = P_0 + P_c - P_x$. Replacing ΔP in Eq. (3) describes the transient flow, but instead of explicitly writing P_x and P_c it is convenient to rewrite these as a function of geometrical parameters.

Considering an isothermal compression of the air inside the microchannel, P_x can be approximated by

$$P_x(x) = P_0\frac{L}{L-x} \tag{4}$$

where L is the total length of the channel. Notice that Eq. (4) shows that P_x can be determined without any dedicated pressure sensor by measuring the atmospheric pressure and the position of the fluid column. Furthermore, at the rest position $P_x(L_f) = P_0 + P_c$, and then the capillary pressure P_c can also be calculated as

$$P_c = P_0\frac{L_f}{L-L_f} \tag{5}$$

Using Eqs. (4 and 5) and replacing $\frac{\Delta P}{x}$ in Eq. (3) the mean velocity $u(x)$ is

$$u = \frac{D}{2((1/n)+3)\left(\frac{D}{4k}\frac{P_0}{(1-(L_f/L))}\frac{L_f-x}{x(L_t-x)}\right)}^{1/n} \tag{6}$$

and this equation can be used to calculate n and k, by independently measuring P_0 and the geometrical parameters D, L and L_f.

3. Experimental details

To analyze the transient capillary flow of a power law fluid, we have used a microfluidic device featuring a custom design with a long serpentine packaged in a 10 mm × 10 mm × 1 mm glass chip. The microchannels with a 40 μm width and a 15 μm depth were built using photolithography and wet etching techniques on soda lime glass wafers. After bonding to a seconds glass wafer, individual chips were diced opening a side inlet where the testing fluids drops are then placed. The channels hydraulic diameter D_h was calculated after [15] for an isotropically etched cross sections, obtaining $D_h = 20.7$ μm.

Whole blood and a diluted water based wall varnish *(1:10 – Varnish:DI water)* were selected as test power law fluids, and DI water as a reference Newtonian fluid. The fluids rheology were determined using a commercial Brookfield Rotational Microviscometer with a sample volume of 250 μl for shear rates between 10 s^{-1} and 250 s^{-1}.

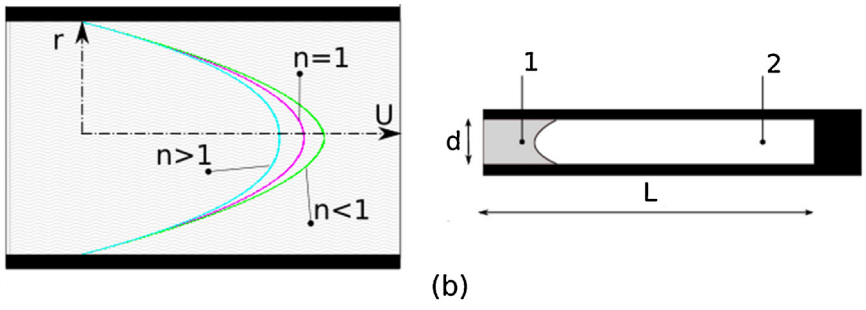

Fig. 1. Schematic of the power law fluid flow inside a microchannel. (a) A power law constitutive equation is defined featuring the viscosity constant k and the exponent n. (a) The parabolic velocity profile is stretched or flattened depending on the exponent n. (b) Schematic of a fluid entering closed channel by capillary pressure. Region 1: fluid, region 2: trapped gas.

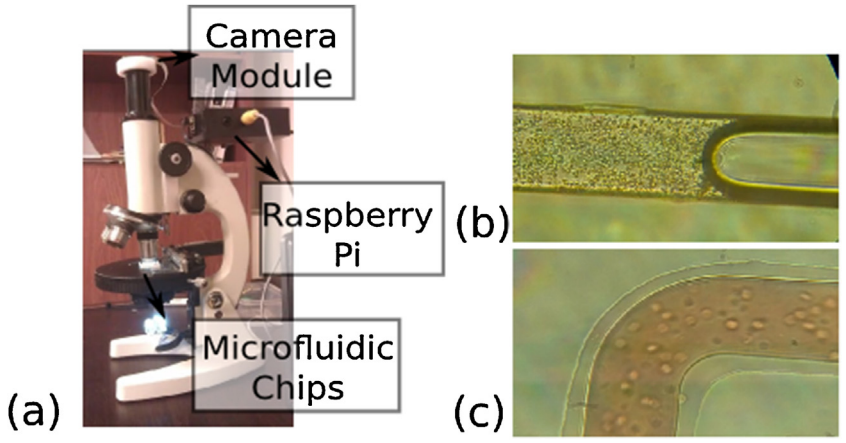

Fig. 2. (a) μPIV setup using a monocular microscope, a Raspberry PI Single Board Computer and a Full HD Camera Module. (b) Snapshot of DI water capillary filling featuring the meniscus and the tracing particles used. (c) Snapshot of whole blood and the red globe cells that were used as tracing particles.

3.1. μPIV and velocity profiles

We have implemented a low cost μPIV, *(Micro Particle Image Velocimetry)* [14] method to determine de velocity profile from a sequence of images. The system features a monocular microscope with a 45× objective lens, a Raspberry Pi Single Board Computer and its dedicated Raspberry Cam Module [16] (maximum resolution: 0.25 μm/pixel, field of view: 350 m × 350 m) (Fig. 2-a). The video was then processed with a custom made image processing software written in Python using the Open Computer Vision Library [17].

The microfluidic chips were fixed under the microscope and fluid drops were placed using a 10 μl micropipette. Polymer microspheres (*Nanosphere 900 nm ∅, Duke Scientific Corporation*) were added to DI water/Varnish as tracing particles to capture the fluid motion (Fig. 2b). For whole blood, the red blood cells motion was traceable and no additional particle was needed (Fig. 2c).

The velocity profile was calculated, and the power law index was obtained by fitting Eq. (2).

3.2. Capillary filling in a single channel

A microviscometer was built using a commercial USB microscope attached to a temperature controlled chip holder (Fig. 3a). Videos were recorded at 10 frames per second using LEDs arrays as a light source. The lower magnification and greater field of view, compared to the μPIV setup, allowed to record the fluid motion since the drop was placed until it stopped at the rest position L_f. The frames were analyzed with a dedicated image processing software through background substraction and noise filtering operations, thus obtaining x and t framewise. The distance between consecutive channels was used to calibrate the length scale by measuring the length in pixels with the USB Microscope and the length in μm using a Nikon Eclipse L200 Optical microscope, obtaining a spatial resolution of 8 μm/pixel. The velocity $u = dx/dt$ was calculated by smoothing the datasets and when it dropped under 1 μm/s the fluid was considered to be at rest. Given the measured spatial resolution, this velocity criteria implied a subpixel resolution for L_f. Finally, the viscosity parameters n and k were determined by plotting u vs. x and fitting Eq. (6)

4. Results

DI water, whole blood and the white varnish were measured in a Brookfield Rotational Microviscometer. The viscosity values for different shear rates, plotted in a log–log scale (Fig. 4), show a decreasing line for blood and varnish. Following Eq. (1), the slope of that line equals to $(n-1)$. The line fit gives $n = 0.92$ for Varnish and $n = 0.79$ for blood, while for DI water $n = 0.99$ is close to 1 as expected for a Newtonian fluid.

Fig. 5a shows a snapshot of the μPIV experiment with the overlapped velocity field averaged over 100 frames. To simplify the velocity profile calculation, the image was first rotated under the

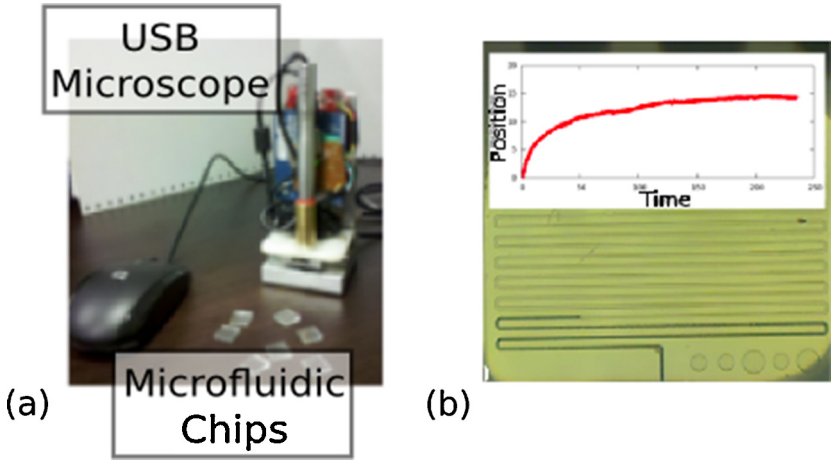

Fig. 3. (a) The USB microscope setup with a temperature controlled holder to insert to analyze the fluid's transient flow inside the microchannel. (b) An image from the USB microscope of the fluid entering the channel. The inner plot shows how instant position of the fluid column as a function of time.

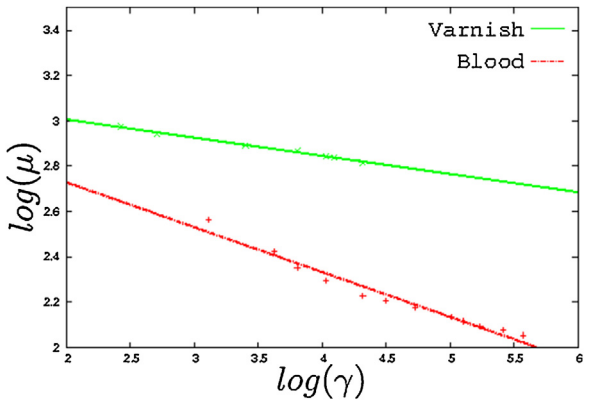

Fig. 4. Fluid viscosity as a function of the shear rate measured with a commercial Brookfield Rotational Microviscometer. In a power law fluid, the slope in a log–log scale is $n-1$. It can be seen that blood has a lower n as its slope is steeper negative.

microscope and corrected via software to align the channel over x-axis and so the velocity field had that dominant component. Although the hydrophilic surface of the channel ensures a no slip condition on the channel walls, a non-zero velocity is obtained as a consequence of the window size used to smooth the velocity profile in the μPIV algorithm.

The plots of the profiles (Fig. 5b) were fit near the center of the channel with Eq. (2) using a nonlinear power function $f(x) = A * x^B + C$ obtaining $B = 1.98$ for DI Water, $B = 2.09$ for varnish and $B = 2.16$ for blood. As expected, the parabolic profile is flattened as the exponent n decreases. From Eq. (2) $B = 1 + 1/n$, then with $n = 1.02$ for DI water, $n = 0.92$ for varnish and $n = 0.84$ for blood.

The transient flow experiments were done controlling the chip holder temperature to 20 °C. The drop was placed on the side of the chip and the images were processed as shown in Fig. 6 obtaining x vs. t and u vs. x plots.

The exponent n is calculated by linear fitting a log–log plot of u vs. $\frac{L_f - x}{x(L-x)}$ (Fig. 6) where from Eq. (6) it can be seen that the slope of the line is $1/n$. With n known the parameter k is determined by fitting u vs. $\left(\frac{L_f - x}{x(L-x)}\right)^{1/n}$. Performing the experiments we obtained $n = 1.02$, $k = 0.98$ for DI Water, $n = 0.91$, $k = 19.8$ for the varnish and $n = 0.81$, $k = 3.70$ for whole blood.

The comparison of the viscosity parameters obtained with different experiments is explicitly listed in Table 1. Although it was expected that they match quantitatively, it is remarkable that a μPIV experiment with a sub-U$S 200 setup can provide qualitative and quantitative information about the velocity profiles and non-Newtonian behavior of power law fluids.

On the other hand, the single channel microfluidic chip has proven to be a very accurate sensor with costs dropping under $1 per chip and requiring only an embedded system that capture and process a videofeed. Therefore, the single channel capillary microfluidic system is a good candidate to integrate a point of care device that measures blood viscosity for clinical diagnosis and screening.

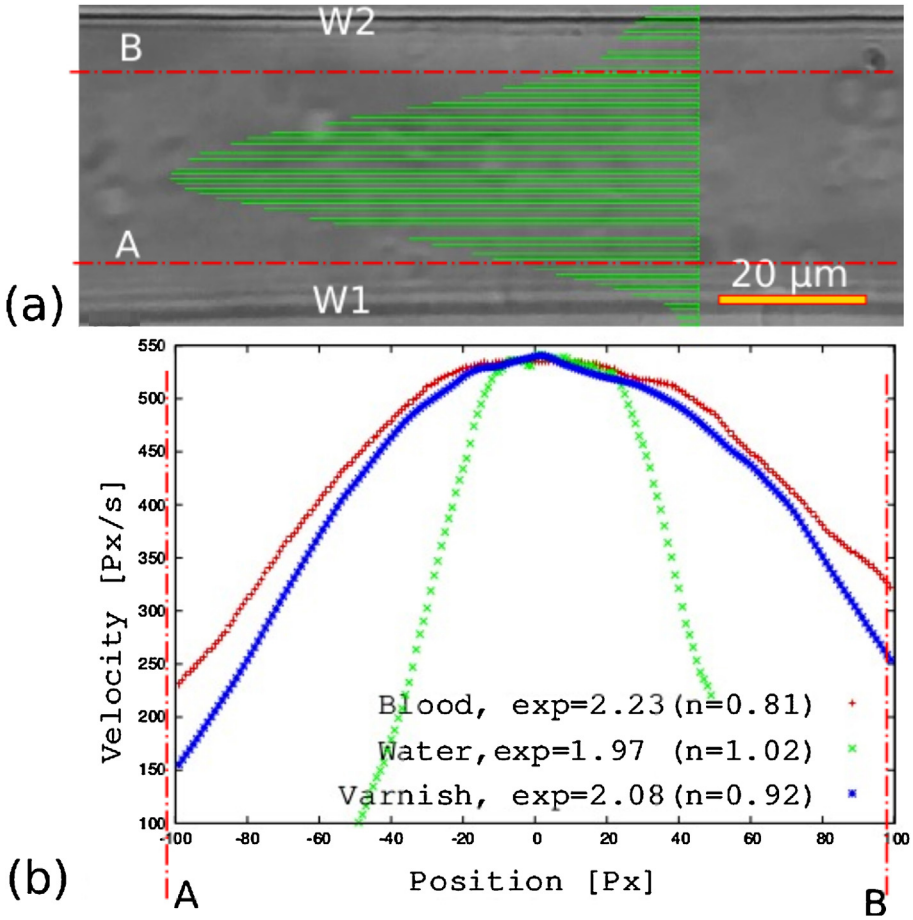

Fig. 5. (a) Grayscale image of the microchannel with an overlapped velocity profile (channels walls marked as W1 and W2). The velocity profile, averaged over 100 frames, is drawn at the middle for visualization purposes. (b) Velocity profiles near the center of the channel (between the A and B lines) for Di Water, Varnish and Blood were obtained by averaging 300 frames (10 seconds of video). Velocities absolute values were normalized to compare the shape of the profiles. As expected, the profile is flattened around the center of the channel as the exponent n decreases. The non-zero velocity at the channel wall is a consequence of the windows size used to smooth the profile.

Table 1
Power law viscosity parameters obtained with different experiments. The exponent n values match compared to the commercial rotational device for both low cost μPIV system and the transient capillary flow concept.

Sample	μPIV	Single channel		Rotational	
	n	n	k [cP]	n	k [cP]
DI Water	1.00 ± 0.03	1.02 ± 0.02	0.98 ± 0.05	0.98 ± 0.01	1.01 ± 0.01
Varnish	0.91 ± 0.03	0.92 ± 0.02	19 ± 2	0.92 ± 0.01	23.5 ± 0.5
Blood	0.80 ± 0.03	0.81 ± 0.02	3.7 ± 0.2	0.78 ± 0.03	3.2 ± 0.1

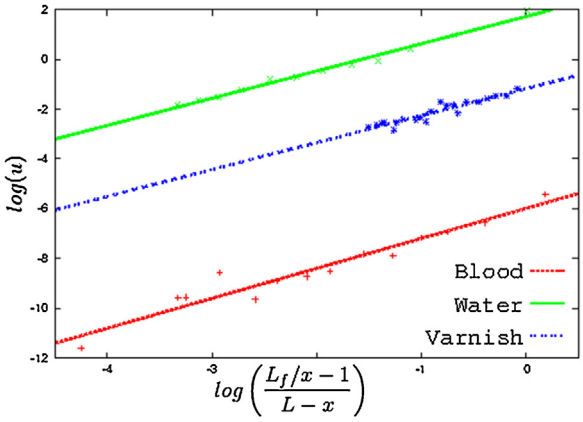

Fig. 6. u vs. $\frac{L_f - x}{x(L-x)}$ plots in log–log scale for water, varnish and whole blood. The linear fit slope gives has the information of the power law parameter n.

5. Conclusions

We have proposed and tested techniques to measure the parameter k and exponent n of power law fluids with a sample volume of 10 μl. By using a single channel microfluidic chip with a side inlet and a close end geometry, we solved the equations for the power law pipe flow and obtained explicit expressions for the velocity profile and the mean velocity of the fluid column across the channel.

A very low cost μPIV experimental set up was implemented and we measured the velocity profile of blood, varnish and DI water, from where we obtained the exponent n according to the expected behaviors for Newtonian and power law fluids.

We have built glass microfluidic chips and registered the transient capillary flow of a fluid drop in an hydrophilic microchannel. The mean velocity analysis of the same fluids were done with an inexpensive embedded system with a USB Microscope and image processing software. This second method showed a consistent result for the exponent n, as well as the parameter k. The viscosity values agreed to those obtained with a commercial rotational microviscometer, validating the single channel design as a microviscometer for power law fluids.

The main advantage of the proposed system is the low cost of the chip and the simplicity of the sensor. Therefore, setting the waypoint towards a point of care microviscometer with disposable chips for clinical purposes in neonatology and rapid cardiovascular screening.

Acknowledgements

The authors would like to acknowledge the support of Consejo Nacional de Actividades Cientficas y Tcnicas (CONICET) and the Comisin Nacional de Energa Atmica (CNEA) for the resources provided to develop this work.

References

[1] Brookfield Engineering, Wells-Brookfield Cone-Plate Microviscometer, http://www.brookfieldengineering.com/.
[2] C. Pipe, G. McKinley, Microfluidic rheometry, Mech. Res. Commun. 36 (2009) 110–120.
[3] B. Weiss, M. Heinisch, E. Reichel, B. Jakoby, Driving modes and material stability of a double membrane rheometer and density sensor, J. Sens. Sens. Syst. (2013) 19.
[4] P. Guillot, P. Panizza, J.-B. Salmon, M. Joanicot, A. Colin, Viscosimeter on a microfluidic chip, Langmuir 22 (2006) 6438–6445.
[5] O. Gaifee, B. Cretin, W. Boireau, C. Baudouy, J.P. Vairac, Optimized microviscosimeter for detection and characterization of biological vesicles, J. Phys. D: Appl. Phys. 41 (41) (2008) 135504, http://dx.doi.org/10.1063/1.1326844 http://link.aip.org/link/?APL/77/4040/1.
[6] J. Chevalier, F. Ayela, Microfluidic on chip viscometers, Rev. Sci. Instrum. 79 (2008).
[7] N. Srivastava, R.D. Davenport, M.A. Burns, Nanoliter viscosimeter for measuring blood plasma, Anal. Chem. 77 (2005) 383–392.
[8] N. Srivastava, M.A. Burns, Analysis of non-Newtonian liquids using a microfluidic capillary viscosimeter, Anal. Chem. 78 (2006) 1690–1696.
[9] N. Morhell, H. Pastoriza, A single channel capillary microviscometer, Microfluid. Nanofluid. 15 (4) (2013) 475–479.
[10] N. Morhell, H. Pastoriza, A discussion of channels designs in microfluidic chips for viscosity sensors, Proceedings of the 3rd European Conference on Microfluidics. http://www.microfluidics2012.eu/74.php.
[11] H.A. Barnes, J.F. Hutton, An Introduction to Rheology, vol. 3, Elsevier, 1989.
[12] R.B. Bird, W.E. Stewart, E.N. Lightfoot, Transport Phenomena, John Wiley & Sons, 2007.
[13] M.M. Molla, S.G. Moulic, et al., Fully-developed circular-pipe flow of a non-Newtonian pseudoplastic fluid, Univers. J. Mech. Eng. 1 (2) (2013) 23–31.
[14] J.G. Santiago, S.T. Wereley, C.D. Meinhart, D. Beebe, R.J. Adrian, A particle image velocimetry system for microfluidics, Exp. Fluids 25 (4) (1998) 316–319.
[15] N.-T. Nguyen, A. House (Eds.), Fundamentals and Applications of Microfluidics, 2006, pp. 37–38.
[16] Raspberry Pi Foundation, Raspberry Pi Camera Module, http://www.raspberrypi.org/products/camera-module/.
[17] Intel Corporation, Willow Garage, itseez, Open Source Computer Vision, http://www.opencv.org.

Biographies

N. Morhell obtained a M.Sc. degree in Technological Physics from Instituto Balseiro in 2010 and is currently a PhD Student (Physics) and teacher assistant in Instituto Balseiro. He has worked in microfluidic based sensors involved in microchannels fabrication methods, optical sensors and image analysis, and more recently in technology transfer project. In 2012 he got the MIT's Technology Review TR35 award for young innovators in Argentina and Uruguay. He is currently interested in bringing lab on chip technologies to commercial stages.

H. Pastoriza received his PhD degree in Physics from Institutbo Balseiro in 1994 and has attended post doctoral positions in Leiden Univerisity and Neuchâtel University. He is currently Principal Researcher in CONICET, Researcher in CNEA, and Professor in Instituto Balseiro. He has more than 50 publications in Condensed Matter Physics, Applied Physics and Microsensors. Since 2002 he has been involved in the development of microelectromechanical systems for superconductivity research, satellite sensors and biomedical sensors.